PCCP

ROYAL SOCIETY OF CHEMISTRY

PAPER

Cite this: *Phys. Chem. Chem. Phys.*, 2022, **24**, 883

Evidence for surface effects on the intermolecular interactions in Fe(II) spin crossover coordination polymers†

Thilini K. Ekanayaka, *[a] Hannah Kurz, [b] Kayleigh A. McElveen, [c] Guanhua Hao,[ad] Esha Mishra,[a] Alpha T. N'Diaye, [d] Rebecca Y. Lai, [ce] Birgit Weber [b] and Peter A. Dowben [a]

Received 16th September 2021,
Accepted 3rd December 2021

DOI: 10.1039/d1cp04243b

rsc.li/pccp

From X-ray absorption spectroscopy (XAS) and X-ray photoemission spectroscopy (XPS), it is evident that the spin state transition behavior of Fe(II) spin crossover coordination polymer crystallites at the surface differs from the bulk. A comparison of four different coordination polymers reveals that the observed surface properties may differ from bulk for a variety of reasons. There are Fe(II) spin crossover coordination polymers with either almost complete switching of the spin state at the surface or no switching at all. Oxidation, differences in surface packing, and changes in coordination could all contribute to making the surface very different from the bulk. Some Fe(II) spin crossover coordination polymers may be sufficiently photoactive so that X-ray spectroscopies cannot discern the spin state transition.

1. Introduction

Iron(II) spin crossover materials, which exhibit spin switching between a low spin (LS, $S = 0$) and a high spin (HS, $S = 2$) state upon an external stimulus often show cooperative effects, *i.e.* mediated through intermolecular interactions. Such cooperative effects are usually the reason for abrupt spin state transitions and can result in the occurrence of hysteresis in the spin state transition, with thermal cycling, thus bistability phenomena with different transition temperatures in the heating and the cooling mode.[1–10] Furthermore, such intermolecular interaction between the spin crossover molecules can also affect the spin transition temperature.[1,7,11–22] Therefore, the characteristic spin state transition temperature and associated hysteresis of the spin crossover complex at the surface of a crystallite may differ from the bulk material because of the differences in the environment.[14,22–24] The effect of intermolecular packing can also occur with spin crossover coordination polymers as well, now shown for the coordination polymers $[Fe(L1)(bipy)]_n$ (where L1 is a N_2O_2 ligand bearing a phenazine fluorophore and bipy = 4,4′-bipyridine)[24] and $[Fe(Htrz)_2(trz)](BF_4)$,[25] although complex steric effects tend to be more likely.[7,13] Further cementing the role of local coordination are a number of experiments that have shown that the choice of solvent affects the spin state transition.[26–36]

The question as to whether changes in a surface-to-volume ratio influence device performance becomes important now that ultrathin film nonvolatile memory devices have been fabricated from spin crossover complexes.[37–39] If the surface coordination perturbs the spin state transition, this could influence the overall spin crossover, in the thin film limit,[22,24] because as film thickness decreases, the surface-to-volume ratio increases. Such surface effects could have a profound effect on molecular device performance.[39] For spin crossover coordination polymers, the necessary thin films for scalable memory devices implicates thin film fabrication from solution *via* drop casting, spin coating, or printing[13,33,39–41] as the most practical approach. In the thin film limit, however, both surfaces and the choice of solvent may affect the spin crossover characteristics. Yet a deep understanding of the perturbations to the spin state occupancy with temperature, as a result of the surface or choice of solvent, how it affects the bistability remains far from understood for the spin crossover coordination polymers, especially if different families of spin crossover complexes are discussed. Here we compare the surface properties of two 4,4′-bipyridine (bipy) based and 1,2-bis(4-pyridyl)ethylene (bpee) based Fe(II) spin crossover coordination

[a] *Department of Physics and Astronomy, University of Nebraska, Jorgensen Hall, Lincoln, NE 68588-0299, USA. E-mail: thiliniek@huskers.unl.edu*
[b] *Inorganic Chemistry IV, University of Bayreuth, Universitätsstrasse 30, NW I, 95447 Bayreuth, Germany*
[c] *Department of Chemistry, University of Nebraska, Hamilton Hall, Lincoln, NE 68588, USA*
[d] *Advanced Light Source, Lawrence Berkeley National Laboratory, Berkeley, CA 94720, USA*
[e] *Nebraska Center for Materials and Nanoscience, University of Nebraska-Lincoln, Voetle-Keegan Nano Center, Lincoln, NE 68588, USA*

† Electronic supplementary information (ESI) available. See DOI: 10.1039/d1cp04243b

polymers (polymers with Schiff base-like ligands) with the much studied $[Fe(Htrz)_2(trz)](BF_4)$ coordination polymer.

It has already been acknowledged that different measurements of a transition in the spin state of Fe(II) molecular systems are very dependent on the measurement technique.[22,24,42] More recently, an understanding has emerged that the surface of even a small crystallite of a spin crossover complex can exhibit very different properties from the bulk.

The problem with ascertaining the importance of the surface is that surface sensitive spectroscopies, like X-ray absorption spectroscopy in the total electron yield mode and X-ray photoemission, can perturb the spin state if the spin crossover molecule is photoactive or easily perturbed by the secondary electron current generated by the incident X-ray flux. Light and X-ray induced spin state switching, known as light-induced excited spin-state trapping (LIESST),[43–51] and soft X-ray-induced excited spin state trapping (SOXIESST)[52,53] usually occurs well below the transition temperature where the low spin (LS) state is dominant, but not always so.[43,44,54–58] Photochromic effects are known and can occur in the vicinity of room temperature if there is a photoactive ligand that can be switched by light.[43,44,54–58] Hence, there are spin crossover molecules switchable by light, which can cause a mixed spin state or high spin state over a wide range of temperatures. As we show here, the complication that optical and X-ray characterization techniques can activate spin state switching from the low spin (LS) state to high spin (HS) state needs to be considered along with possible surface effects.

2. Experimental section

Schematic diagrams of $[Fe(L1)(bipy)]_n$, $[Fe(L2)(bipy)]_n$, $[Fe(L3)(bpee)]_n$, and $[Fe(Htrz)_2(trz)](BF_4)$ are given in Fig. 1 and named as molecule **1**, **2**, **3**, and **4**, respectively. The $[Fe(L1)(bipy)]_n$ polymer was synthesized as described elsewhere.[24,59] The $[Fe(L2)(bipy)]_n$ was synthesized as described previously,[60,61] while $[Fe(L3)(bpee)]_n$ was synthesized as reported in Lochenie *et al.*[62] $[Fe(Htrz)_2(trz)](BF_4)$ was synthesized as described in Kroeber *et al.*[63] whereby a 3 M solution of 1,2,4-triazole (99%, Alfa Aesar, Haverhill, MA) in anhydrous ethanol (200 proof, Aldrich, St. Louis, MO) was added at 30 μL min^{-1} while stirring to a 0.5 M solution of iron(II) tetrafluoroborate hexahydrate $(Fe(BF_4)_2 \cdot 6H_2O$, 97%, Aldrich, St. Louis, MO) in anhydrous ethanol. The resulting mixture was stirred for an additional hour and then was left overnight. The supernatant was collected *via* filtration and washed using ethanol three times. The resulting $[Fe(Htrz)_2(trz)](BF_4)$ was allowed to dry.

The X-ray absorption spectroscopy (XAS) measurements were performed on coordination polymers **1**, **2**, **3**, and **4** at the bending magnet beamline 6.3.1, at Advanced Light Source at Lawrence Berkley National Laboratory. The photon flux was in the region of 1.16×10^4 photons·s^{-1} μm^{-2} in the two-bunch mode. As in previous studies, the total electron yield mode was used to measure the absorption across the Fe $2p_{3/2}$ (L_3) edge. The magnetic susceptibility measurements were taken for complex **1**, complex **2**, and complex **3** using a Quantum Design MPMS-XL5 superconducting quantum interference device (SQUID) magnetometer under an applied field of 0.5 T in the sweep mode in the temperature range of 300 K to 400 K and 150 K to 300 K, respectively, to confirm the expected spin crossover behavior for the freshly prepared samples.[64] Magnetometry data for complex 4 was collected using a Quantum Design VersaLab 3 Tesla cryogen-free vibrating sample magnetometer (VSM) at an applied magnetic field of 1 T from 300 K to 400 K. For the XAS and X-ray photoemission spectroscopy (XPS) measurements, for complex **1** and **4** the XAS and XPS measurements were taken from 300 K to 400 K, while for complexes **2** and **3**, the measurements were done between 150 K to 300 K. For XAS the samples were allowed to equilibrate for 10 to 15 minutes while for XPS the samples were allowed to equilibrate to the set temperature for 2 hours.

Temperature-dependent X-ray photoemission spectroscopy (XPS) measurements were taken using non-monochromatized

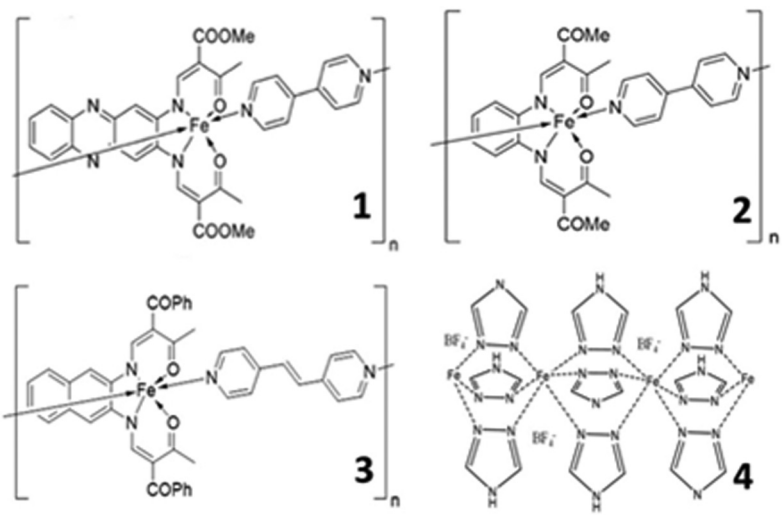

Fig. 1 A schematic representation of spin crossover coordination polymers discussed in this work: **1** – $[Fe(L1)(bipy)]_n$, **2** – $[Fe(L2)(bipy)]_n$, **3** – $[Fe(L3)(bpee)]_n$, and **4** – $[Fe(Htrz)_2(trz)](BF_4)$.

Al K_α X-ray source, with photon energy of 1486.6 eV, and a SPECS PHOIBOS 150 energy analyzer with 20 eV pass energy.[24,65] The samples were mounted on copper conducting tape compatible with ultrahigh vacuum and the photoelectrons were collected normal to the sample. For XAS the samples were mounted on vacuum compatible carbon tape. Both the XAS and XPS measurements shown here are reproducible, with the experiments repeated several times on fresh samples (some of this data is shown in the ESI,† as Fig. S1–S3). Sample degradation/damage of organic molecules, due to X-ray influence is known, and here the samples were only exposed to X-rays while taking data and the X-ray influences reduced in some experimental trials, though at a cost of signal to noise and resolution. Here, each measurement has been done on fresh samples to avoid any complication that could be caused by sample degradation and thermal training effects. The reversibility of temperature dependent state transition tends to exclude significant sample degradation for complexes **1**, **2** and **3** during the course of these measurements.[24] Surface oxidation and photoexcitation processes as may occur for **3** and **4** could disguise X-ray or electron induced degradation (as discussed below), but such effects have not been noted in the many prior studies of $[Fe(Htrz)_2(trz)][(BF_4)]$.[43,44]

3. The coexistence of two spin states at elevated temperatures in X-ray absorption spectroscopy

The observed spin crossover behavior of iron(II) complexes, or the coexistence of two spin states, may change depending on the type of characterization techniques used.[24,43,65] Magnetometry and XAS are the most frequently used characterization techniques of the spin state of spin crossover complexes,[7,12–15,22,24,35,42,65–74] but the results do not always show the same spin transition behavior. The spin transition temperature obtained from X-ray absorption spectroscopy is always lower than the transition temperature ($T_{1/2}$) obtained from magnetometry measurements.[24,42,44] X-ray photoemission spectroscopy (XPS) has recently been used to probe the spin transition temperature.[24] This adds to the picture that the Fe 2p core level spectra, taken by the X-ray core level photoemission, is sensitive to the Fe^{2+} spin transition.[24,54,75–78]

Fig. 2 shows the Fe 2p (L-edge) X-ray absorption spectra (XAS) of Fe^{2+} spin crossover coordination polymers of **1** (Fig. 2a), **2** (Fig. 2b), **3** (Fig. 2c), and **4** (Fig. 2d), respectively. As XAS measures the transition of electrons from occupied Fe 2p orbitals to Fe 3d empty orbitals, the XAS spectra indicates the Fe 3d weighted empty molecular orbitals. The ligand field splits the Fe 3d orbitals into t_{2g} and e_g orbital levels which can be seen in the XAS spectra. As is true for d^6 spin crossover systems, at low spin state (LS) the six 3d electrons occupy the t_{2g} orbitals in pairs leaving the e_g orbitals empty, whereas in high spin e_g orbitals are partly filled leaving t_{2g} subsequently partly depopulated.[79] As reported before,[24] in the XAS spectra of complex **1** at 300 K, which is the LS state indicated in blue, the major e_g peak is observed around 710 to 711 eV. By changing the temperature from 300 K to 400 K, the XAS spectrum shows a decrease of the peak intensity at 710 to 711 eV and an increase of the corresponding t_{2g} peak at around 709 eV. Similar transitions have been observed in other spin

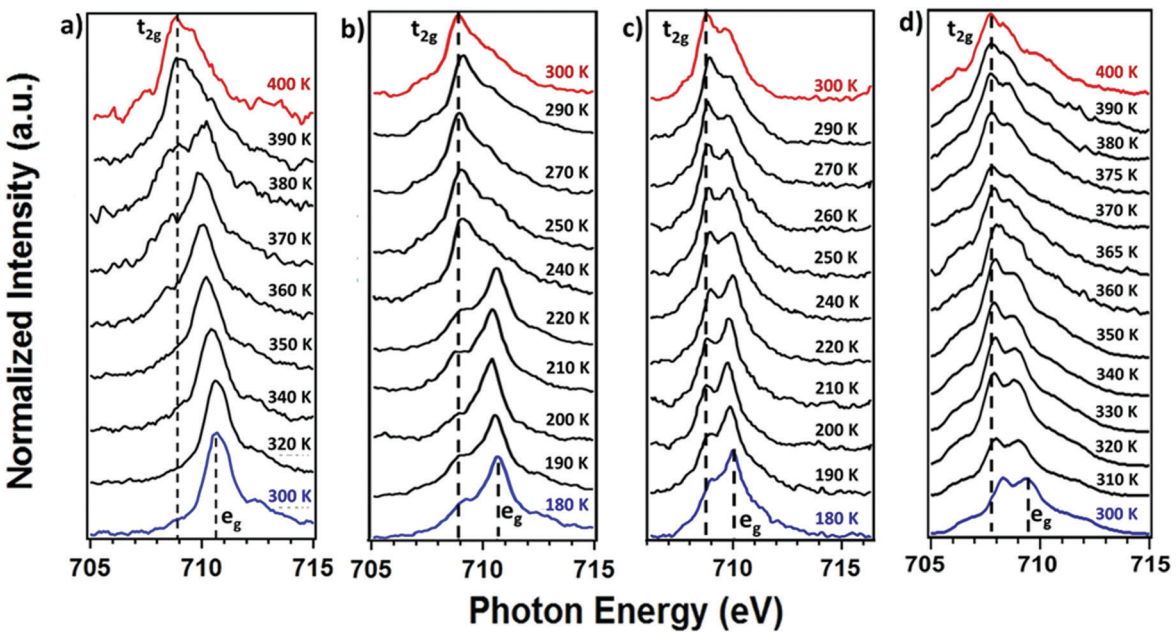

Fig. 2 The temperature-dependent X-ray absorption spectra of spin crossover coordination polymer (a) **1** – $[Fe(L1)(bipy)]_n$, (b) **2** – $[Fe(L2)(bipy)]_n$, (c) **3** – $[Fe(L3)(bpee)]_n$ and (d) **4** – $[Fe(Htrz)_2(trz)](BF_4)$ with increasing temperature. Blue indicates the Fe $2p_{3/2}$ – L_3 edge spectrum of the nominally low spin (LS) state and red indicates the spectrum of the high spin (HS) state, but only do the lower temperature spectra of $[Fe(L1)(bipy)]_n$ exhibit the XAS spectra of the low spin state, without high spin state t_{2g} contributions.

crossover systems.[22,24,37,42,65,69–71,74,80–86] At the lowest temperature, the XAS spectra indicate that complex **1** is in the low spin state, while there is some high spin state fraction indicated in the XAS spectra of complex **2**, **3** and **4**, as indicated in the comparison figure shown in the ESI† (Fig. S4). The trend in the contribution of the high spin state fraction to the XAS spectra of each compound nominally in the low spin state goes as **4** > **3** > **2** > **1** as summarized in the ESI† and Fig. 4.

The X-ray absorption spectroscopies of **2** (Fig. 2b) show a clear spin transition in the temperature region of 180 K to 260 K. The e_g peak and the t_{2g} peak are observed in the same region as for **1**, which is in line with the very similar ligand system. For **3** and **4**, which have different bridging ligands than **1** and **2**, the two prominent XAS peaks are shifted to lower energy photon energies. This indicates that the position of the XAS peaks is strongly influenced by the bridging (axial) ligands, as the equatorial ligand of **1**, **2**, and **3** is very similar. Here, changes in the ligand backbone apparently do not influence the positions of the XAS features. This is in line with results from DFT calculations that also indicate a minor impact of the Schiff base-like ligand backbone on the energies of the d orbitals.[87,88] According to magnetic measurements, at the lowest measurement temperature, all complexes should be almost completely in the LS state. In comparison with **1**, however, **2** (Fig. 2c), **3** (10% HS expected at 180 K according to SQUID measurement) (Fig. 2c), and **4** (Fig. 2d) are not completely in the LS state. As described above, there is a signature of the partially occupied high spin t_{2g} orbitals in the Fe L_3 XAS spectra evident in some t_{2g} intensity at around 704 eV. The spin transition of the system will occur with increasing temperature, and this can be elucidated from the XAS spectra as the peak intensity of e_g decreases and the t_{2g} peak intensity around 704 eV increases. This spin crossover system obtains complete HS occupancy at higher temperatures. A clear spin transition is also seen for complex **2** (Fig. S2, ESI†) and **3** (Fig. S3, ESI†) with decreasing temperature.

It is also important to note that there are differences between the XAS spectra taken with increasing and decreasing temperature, even at an identical temperature. As seen in the ESI† (Fig. S5, ESI†) XAS spectra do not overlay perfectly as a result of hysteresis in the spin state occupancy.

Clearly, while the high spin state spectra of **1** (Fig. 2a), **2**, (Fig. 2b), **3** (Fig. 2c) and **4** (Fig. 2d) are very similar, the nominally low spin state spectra (blue) are not. So while the XAS spectra indicate that the high spin state occupancy is close to zero for molecule **1**, below the transition (300 K) there is about 20% high spin state occupancy for **2** but more than 60% high spin state occupancy for **3** and **4**.

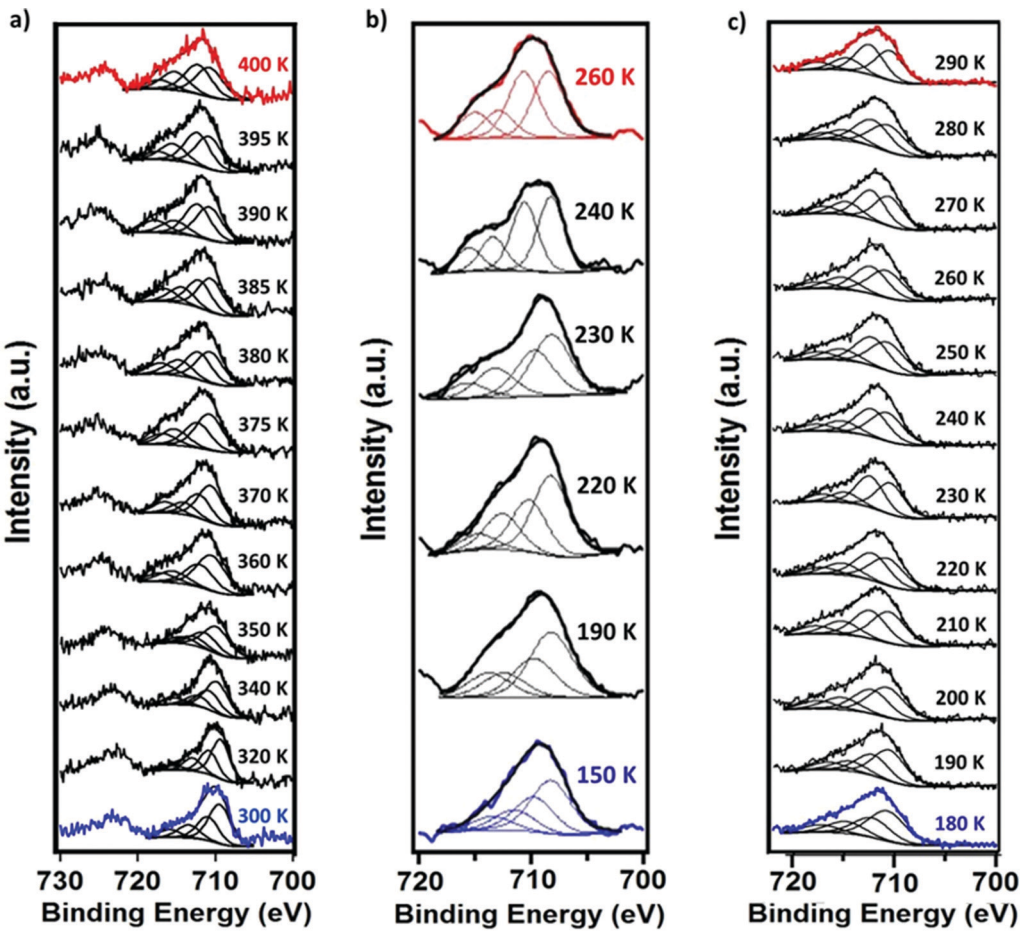

Fig. 3 Temperature-dependent X-ray photoemission spectra of (a) **1** – $[Fe(L1)(bipy)]_n$, (b) **2** – $[Fe(L2)(bipy)]_n$, and (c) **3** – $[Fe(L3)(bpee)]_n$. The spectrum in red is representative of the high spin state while the spectrum in blue is representative of the low spin state.

Surface effects have been implicated for molecule **1**,[24] and such surface effects do much to explain the differences between magnetometry and X-ray absorption regarding the temperature dependence of the HS state and LS state spin state occupancy for **1**. Surface oxidation is not implicated here or in the prior studies of **1**,[24] because of spin state reversibility with temperature and because the Fe 2p core level binding energies, discussed below, do not indicate molecular decomposition nor oxidation of the Fe^{2+} core in **1**. Because at low temperatures, the X-ray absorption spectra of **2**, (Fig. 2b), **3** (Fig. 2c) and **4** (Fig. 2d) are not characteristic of the low spin state (*i.e.* not similar to the blue spectrum in Fig. 1a), there is every indication of a mixed spin state or high spin state in the X-ray absorption, even at the lowest temperatures for **2**, **3**, and **4**. While this can also be the result of surface effects, implicated in the case of **1**, surface oxidation and photochromic effects must be considered as well.

4. X-ray photoemission spectroscopy and surface oxidation

The temperature dependent X-ray photoemission spectroscopy measurements of **1**, **2**, and **3** are shown in Fig. 3(a), (b) and (c) respectively. The Fe $2p_{3/2}$ core level binding energy is around 709.5 eV for **1**, 708 eV for **2** and 711 eV for **3**. Studies done on these different spin crossover systems are generally consistent with the Fe $2p_{3/2}$ core level binding energy values obtained for these spin crossover systems.[24,44,53,65,75–79,89–91] Binding energies of 709.5 eV for $[Fe(L1)(bipy)]_n$,[24] 709.3 eV for $[Fe(H_2B(pz)_2)_2(phen^*)]$ (where (phen*) = a diarylethene-functionalized phenanthroline ligand),[77] 709.5 eV for $[Fe(HB(trz)_3)_2]$ (where $HB(trz)_3$ = tris(1*H*-1,2,4-triazol-1-yl)borohydride),[53] 709.9 eV for $[Fe(phen)_2(NCS)_2]$ powder,[90] and 709.3 eV for $[Fe(phen)_2(NCS)_2]$ films[89] have been observed. Accordingly, the higher binding energies for molecule **3** (roughly 711 eV) may be indicative of surface oxidation. Surface oxidation could also affect the XAS spectra, so that the apparent incomplete SCO in XAS is a result of surface oxidation and could explain why the peak energies are shifted in XAS for **3** (Fig. 2c). Because the Fe $2p_{3/2}$ core level binding energy values obtained for these spin crossover systems **1** and **2** are in line with expectations, for these systems, surface oxidation is unlikely to be the origin for the difference between X-ray absorption and magnetometry, as plotted in Fig. 4a and b. It should be noted that the surface oxidation will add significant uncertainty to the estimates of the high spin state fraction determined from XAS and could obscure evidence of degradation due to the X-ray or photoelectron fluence because of the possibly heterogeneous Fe–O bonding. If the oxidation is not homogeneous, as seems likely, the XPS will be complicated by overlapping multiplet and satellite components in the Fe 2p spectra.[89,92–94]

5. X-ray photoemission spectroscopy and Fe 2p multiplets

The Fe $2p_{3/2}$ of the XPS spectra has a broad core level line width in both systems which indicate that multiplet splitting exists in

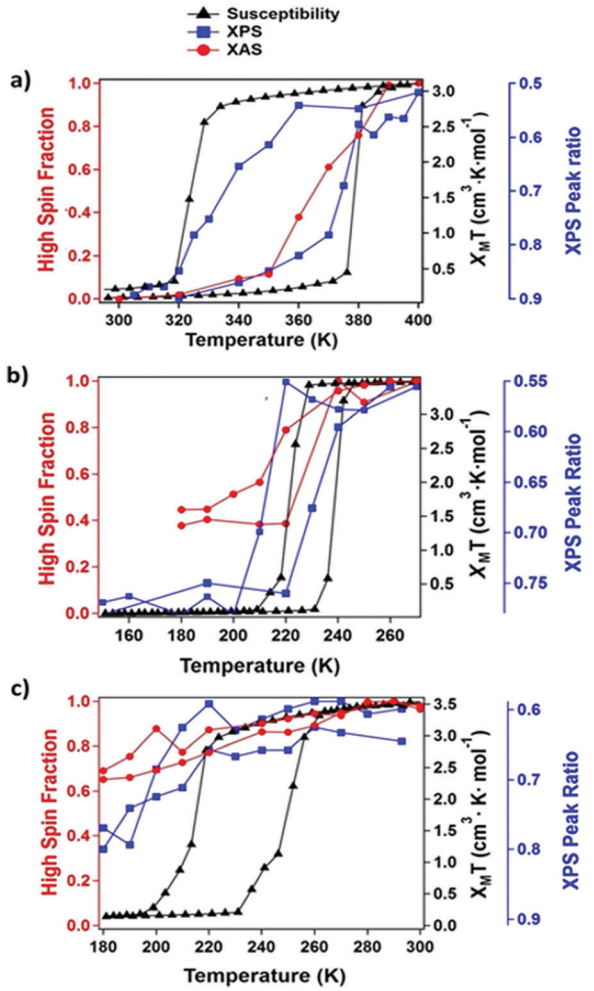

Fig. 4 The molecular magnetic susceptibility (black curve) and the high spin fraction obtained from XAS spectroscopy measurements (red curve) compared with occupancy of the high spin state derived peak ratio (P1/P2 + P3 + P4) of XPS multiplets (blue curve) with respect to temperature for (a) **1** – $[Fe(L1)(bipy)]_n$, (b) **2** – $[Fe(L2)(bipy)]_n$, and (c) **3** – $[Fe(L3)(bpee)]_n$.

the Fe $2p_{3/2}$ core level peak. Multiplet splitting is common for most of the transition metal ions yet changes in the intensities of the multiplets is a good indicator of changes in the spin state of spin crossover molecular complexes.[24,54,65,75–78] The multiplet splitting in the Fe $2p_{3/2}$ core level XPS is significant when there are unpaired Fe spins therefore, in the HS state, the multiplet intensities will be more pronounced.[24,54,58,65,74–77,89–95] In the LS state there will be no unpaired spins, hence multiplet splitting will not be pronounced in LS state.

Multiplet splitting, for the Fe $2p_{3/2}$ core level, was observed for the low spin state of **1**, **2**, and **3** at 300 K, 150 K, and 180 K, respectively. In both complexes, with increasing temperature the Fe $2p_{3/2}$ peak broadens towards the higher binding energy while changing the multiplet peak intensities, that is to say with the higher spin state, the satellite multiplet intensities increase. The relative intensities become redistributed among the multiplets, with changing spin configurations. Similar changes in the satellite Fe $2p_{3/2}$ core level feature intensities have been reported for other spin crossover complexes,[24,54,65,75–78] as noted

above. The change in the intensities of the multiplets can be compared by taking the peak ratio of the first peak in the low binding energy region to the other three components. That is Peak 1 to the sum (Peak 2 + Peak 3 + Peak 4). The Fe $2p_{3/2}$ peak ratios, indicating the change in spin state as extracted from the XPS spectra, are plotted with respect to temperature together with the high spin fraction, as obtained from the XAS spectra, and with magnetic susceptibility data for the spin crossover complexes **1**, **2**, and **3** (Fig. 4a–c).

For XPS, it is difficult to be certain what the electron mean free path is in our samples as these are metal organics and not pure organic films, but the value should be close to what is seen in organic films, or about 4 nm.[96] Given the small kinetic energies the probing depth of XAS will be less,[97] as noted elsewhere.[24] XAS is dominated by secondary electron emission, much of which is peaked at about 50 eV kinetic energy, or the minimum of the electron mean free path.[98–100] Both XAS and XPS are more surface sensitive than magnetometry as schematically shown in Fig. 5. This does much to explain the differences between magnetometry, and the results from XAS and XPS for molecules **1** and **2**, as summarized in Fig. 3.

The magnetometry of **1** gives a 54 K wide hysteresis loop with spin transition temperatures ($T_{1/2}$) on heating and cooling at 378 K and 324 K, respectively.[24] The XPS peak ratio follows the magnetic susceptibility curve, but with a narrower hysteresis and spin transition temperatures (T_{XPS}) for heating and cooling at 373 K and 335 K. The spin transition temperature obtained from XAS (T_{XAS}) for increasing temperature was at 367 K, a lower temperature compared to both the spin transition temperature obtained from magnetometry and XPS, *i.e.* $T_{1/2}$ and T_{XPS} respectively. This change in the hysteresis for **1** has been suggested to be the result of the surface sensitivity of XPS compared to the bulk magnetometry measurement.[24] The shifts seen with XAS derived high spin state fraction with increasing temperature are expected as XAS in the TEY mode is even more surface sensitive than XPS.[24] At the surface there is lower coordination or lower intermolecular interaction compared to the bulk, so the cooperative effects likely differ. With lower coordination, the decrease in cooperative effects should decrease the hysteresis.

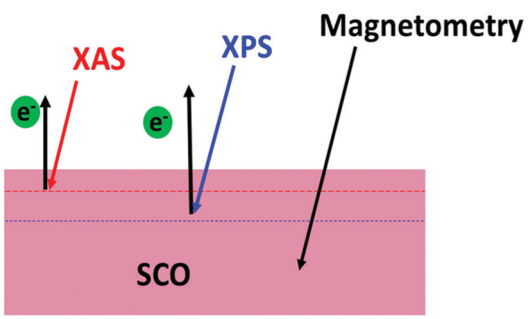

Fig. 5 A schematic to indicate the probing depth of XAS is more surface sensitive than XPS. Both XAS and XPS are surface sensitive tecniques while magnetometry is a bulk technique.

For spin crossover complex **2**, the magnetometry shows some hysteresis in the spin state transition, with transitions at 222 K and 240 K on heating and cooling respectively, *i.e.* the hysteresis is 18 K wide. The XPS peak ratio shows hysteresis and follows the magnetic susceptibility data of **2** but there are differences, nonetheless. The XPS peak ratio indicates lower spin state transition temperatures than are evident in magnetic susceptibility data for both heating and cooling. While the transition temperatures seen in XPS have been shifted to lower temperature compared to magnetometry measurements, there is, similarly shaped hysteresis. That the hysteresis temperature width is largely preserved in comparing magnetometry and XPS (in spite of a shift in the transition temperature), with **2** is significantly different than the behavior seen with the very similar spin crossover polymer **1**. High spin occupancy fraction of **2**, determined from the XAS spectra, also shows a hysteresis and is similar to the magnetometry, but the lowest temperature XAS spectra are more characteristic of a mixed spin state with some high spin state fraction. Furthermore, the hysteresis for **2**, determined from the even more surface sensitive XAS, may be smaller than indicated by XPS. The influence of the surface could affect temperature dependence of the spin state, thus influencing the X-ray absorption and X-ray photoemission measurements of **2** as well as **1**. We can infer from the overall spin state transition temperature that **2** has a lower spin state change activation energy than **1** yet spin state transition activation energy ΔH at the surface of **2** must be lower still. The differences in the transition temperature obtained from these different techniques may be due to the difference in the cooperative effects at the surface and bulk for **2**, as is the case for **1**. As noted above, we consider surface oxidation as unlikely to be the origin of these effects and while not excluded, **2** is not yet known for strong photochromic effects well above the LIESST temperature (roughly 50 K).[50]

As the thermal SCO temperature is much lower for **2** compared to **1**, photochromic effects above the LIESST temperature are one possible explanation for the measurement results. Another more likely explanation of the measurement dependent hysteresis data provided is, however, that the surface coordination of **2** differs from **1**. This means that the polymer strands of **1** could be arranged parallel to the particle surface leading to a complete spin crossover, but with differences in the hysteresis width and transition temperatures. In contrast to the situation with **1**, in the case of **2** the polymer strands could be aligned vertical to the particle surface leading to chain ends that are not spin crossover active. These differences between the surface and bulk contributions to XAS and XPS *versus* magnetometry do not apply to **3** and **4**.

For **3**, the magnetometry shows some hysteresis in the spin state transition, with transitions at 217 K and 250 K, but the hysteresis is much diminished in XPS and XAS, even with the consideration that both XAS and XPS indicate a significant high spin state population, even at the lowest temperatures. Among the explanations as to the differences in the spin state transition as seen in XAS and XPS *versus* magnetometry for **3** are that the HS dominates at the surface, to which XAS and XPS

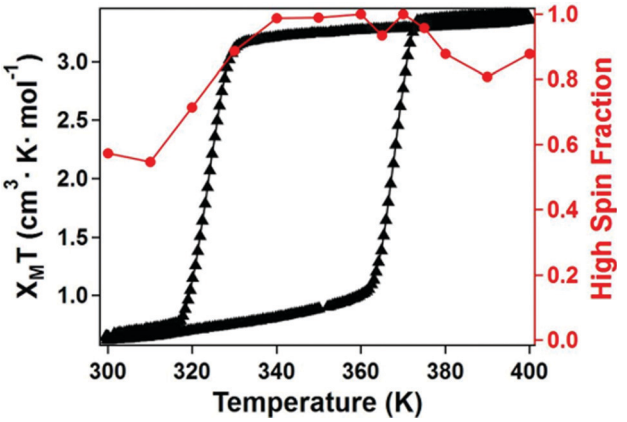

Fig. 6 The molecular magnetic susceptibility (black curve) and the high spin fraction obtained from XAS spectroscopy measurements (red curve) for **4**.

are more sensitive,[24] as noted above, and does so more than for **1** and **2**. This is consistent with the SQUID magnetometry measurements. The SQUID magnetometry measurements, for **3** shows an incomplete SCO with 5–10% high spin fraction at low temperatures, whereas for **1** and **2**, magnetometry shows the material to be more completely in the low state at low temperatures (Fig. 4). As noted above, it is quite possible that the surface of **3** is oxidized as is suggested by the much higher Fe $2p_{3/2}$ core level binding energy seen for **3** than for **1** or **2**. Thus the differences between X-ray photoemission, X-ray absorption and magnetometry for **3** could well be a surface effect, but in the case of **3**, the influence of the surface on the X-ray photoemission, X-ray absorption results is due to surface oxidation, not differences in surface coordination.

6. Photochromic effects in X-ray absorption and X-ray photoemission

The high spin fraction, determined from XAS, for **4** does not follow the magnetometry data (Fig. 6), as noted in detail above. As is clear from the XAS spectra for the **4**, overall these results indicate that the spin crossover transition and the bistability of a spin crossover system can be altered by the characterization techniques, especially for a photoactive species like **4**.[43,44] As noted above and elsewhere, XPS and XAS (in the TEY mode) are surface sensitive techniques[24] due to the limited electron mean free paths in X-ray photoemission, X-ray absorption, while magnetometry is a bulk measurement.

In the case of **4**, it has been well established that this spin crossover polymer is photoactive and thus susceptible to excitations to the high spin state.[43,44] This is a photoactive response in the vicinity room temperature well above the light-induced excited spin-state trapping (LIESST),[43–56] which is typically suppressed above 50 K. To see any changes in the XAS spectra of **4**, as a function of temperature, is actually surprising given the propensity of X-rays to excite **4** into the high spin state[43,44] over a broad range of temperatures including in the vicinity of room temperature and above, and at temperatures far above where the LIESST effect is seen for **2**.[51] Photochromic effects are known and can occur in the vicinity of room temperature if there is a photoactive ligand that can be switched by light[43,44,54–58] and the incident X-rays can suppress identification of a spin state change, even in X-ray diffraction.[101] Photochromic effects are not excluded as influencing the X-ray photoemission and X-ray absorption results for **1**, **2**, and **3**, although we note that strong photochromic effects have not been reported, outside of LIESST effects, for **1**, **2**, and **3**. Photochromic effects are unlikely to be a strong influencing on the X-ray photoemission and X-ray absorption in the temperature range of 300 K to 400 K for **1** because the spin state change is not shifted to lower temperatures with decreasing temperature.

Conclusions

In summary, both the surface and likely changes to the packing, resulting from the choice of solvents affect the cooperativity and hence the temperature characteristics of the spin state transition seen for Fe^{2+} spin crossover polymers as now seen here. The influence of the surface could affect temperature dependence of the spin state, thus influencing the X-ray absorption and X-ray photoemission measurements of **2** as well as **1**, as seen here. In the case of **2**, photochromic effects are not entirely excluded on the basis, although, outside of LIESST effects, photochromic effects have not been reported for **1**, **2**, and **3**.

Surface effects in the form of end groups, packing and molecular coordination but less compelling as origins for influencing the X-ray absorption and X-ray photoemission measurements for **3** and **4**. The large core level binding energies suggest that the X-ray absorption and X-ray photoemission measurements are influenced by surface oxidation of **3**. The X-ray absorption and X-ray photoemission measurements of **4** are very likely affected by the incident X-ray fluence or secondary electron flux generated, but surface effects are not excluded from influence the XAS and XPS measurements of **3** and **4**.

The data provided here suggests that both coordination and packing affect the cooperativity of the spin state change in polymers, but surface contamination and surface oxidation cannot be excluded as a source of a surface perturbation in the case of some Fe(II) spin crossover coordination polymers. Photochromic effects are also possible and indeed we note that photochromic effects may differ at the surface and the bulk. This means that the critical temperatures measured for a spin state transition may depend upon the choice of spectroscopy and the manner of sample preparation, not just the molecular spin crossover complex alone. These issues are now seen to apply to SCO polymers as well and thus while surface effects can affect the measured spin state transition, the measurements themselves may perturb the spin state.

Conflicts of interest

There are no conflicts to declare.

Acknowledgements

This research was supported by the National Science Foundation through NSF-DMR 2003057 [T. Ekanayaka, G. Hao, P. A. Dowben], the Nebraska MRSEC NSF-DMR 1420645 [R. Lai, K. McElveen] and NSF-DMR: 1827690 [E. Mishra, R. Lai]. Use of the Advanced Light Source, Lawrence Berkeley National Laboratory, was supported by the U.S. Department of Energy (DOE) under contract no. DE-AC02-05CH11231. H. K. acknowledges financial support by the FCI (Fonds of the Chemical Industry) and the MINT Lehramt plus. The research was performed in part in the Nebraska Nanoscale Facility: National Nanotechnology Coordinated Infrastructure which supported by the National Science Foundation under award no. ECCS: 1542182 and the Nebraska Research Initiative through the Nebraska Center for Materials and Nanoscience. The authors acknowledge Jeffrey E. Shield and Rifat Mahbub for technical support.

References

1 P. Gütlich, Y. Garcia and H. A. Goodwin, Spin crossover phenomena in Fe(II) complexes, *Chem. Soc. Rev.*, 2000, **29**, 419–427.
2 K. Ridier, G. Molnár, L. Salmon, W. Nicolazzi and A. Bousseksou, Hysteresis, nucleation and growth phenomena in spin-crossover solid, *Solid State Sci.*, 2017, **17**, A1–A22.
3 H. Hang, B. Fei, X. Q. Chen, M. L. Tong, V. Ksenofontov, A. Il'ya and X. Bao, Multiple spin phases in a switchable Fe(ii) complex: polymorphism and symmetry breaking effects, *J. Mater. Chem. C*, 2018, **6**, 3352–3361.
4 P. Guionneau, J. F. Létard, D. S. Yufit, D. Chasseau, G. Bravic, A. E. Goeta, J. A. Howard and O. Kahn, Structural approach of the features of the spin crossover transition in iron (II) compounds, *J. Mater. Chem.*, 1999, **9**, 985–994.
5 P. Gütlich, A. B. Gaspar and Y. Garcia, Spin state switching in iron coordination compounds, Beilstein, *J. Org. Chem.*, 2013, **9**, 342–391.
6 W. Nicolazzi and A. Bousseksou, Thermodynamical aspects of the spin crossover phenomenon, *C. R. Chim*, 2018, **21**, 1060–1074.
7 A. Bousseksou, G. Molnár, L. Salmon and W. Nicolazzi, Molecular spin crossover phenomenon: recent achievements and prospects, *Chem. Soc. Rev.*, 2011, **40**, 3313–3335.
8 G. Molnár, S. Rat, L. Salmon, W. Nicolazzi and A. Bousseksou, Spin crossover nanomaterials: From fundamental concepts to devices, *Adv. Mater.*, 2018, **30**, 17003862.
9 A. Hauser, J. Jeftić, H. Romstedt, R. Hinek and H. Spiering, Cooperative phenomena and light-induced bistability in iron(II) spin-crossover compounds, *Coord. Chem. Rev.*, 1999, **190**, 471–491.
10 G. Félix, W. Nicolazzi, L. Salmon, G. Molnár, M. Perrier, G. Maurin, J. Larionova, J. Long, Y. Guari and A. Bousseksou, Enhanced cooperative interactions at the nanoscale in spin-crossover materials with a first-order phase transition, *Phys. Rev. Lett.*, 2013, **110**, 235701.
11 F. Prins, M. Monrabal-Capilla, E. A. Osorio, E. Coronado and H. S. J. van der Zant, Room-temperature electrical addressing of a bistable spin-crossover molecular system, *Adv. Mater.*, 2011, **23**, 1545–1549.
12 P. Gütlich and H. A. Goodwin, Spin Crossover - An overall perspective, in *Spin crossover in transition metal compounds I*, ed. P. Gütlich and H. A. Goodwin, Springer, Berlin, 2004, vol. 233, pp. 1–47.
13 T. Mallah and M. Cavallini, Surfaces, thin films and patterning of spin crossover compounds, *C. R. Chim.*, 2018, **12**, 1270–1286.
14 J. A. Real, M. C. Muñoz, J. Faus and X. Solans, Spin crossover in novel Dihydrobis(1-pyrazolyl)borate [H2B(pz)2]-containing Iron(II) complexes. Synthesis, X-ray structure, and magnetic properties of [FeL{H2B(pz)2}2] (L = 1,10-Phenanthroline and 2,2'-Bipyridine), *Inorg. Chem.*, 1997, **36**, 3008–3013.
15 P. Gütlich and H. A. Goodwin, *Spin crossover in transition metal compounds II*, Springer-Verlag, Berlin Heidelberg, 2004, vol. 234.
16 Y. Konishi, H. Tokoro, M. Nishino and S. Miyashita, Monte Carlo simulation of pressure-induced phase transitions in spin-crossover materials, *Phys. Rev. Lett.*, 2008, **100**, 067206.
17 J. Linares, J. Nasser, K. Boukheddaden, A. Bousseksou and F. Varret, Monte Carlo simulations of spin-crossover transitions using the two-level model. I: mononuclear single sublattice case, *J. Magn. Magn. Mater.*, 1995, **140**, 1507–1508.
18 A. Bousseksou, G. Molnár, P. Demont and J. Menegotto, Observation of a thermal hysteresis loop in the dielectric constant of spin crossover complexes: towards molecular memory devices, *J. Mater. Chem.*, 2003, **13**, 2069–2071.
19 G. J. Long, F. Grandjean and D. L. Reger, Spin crossover in Pyrazolylborate and Pyrazolylmethane complexes, in *Spin crossover in transition metal compounds I*, ed. P. Gütlich, H. A. Goodwin, Springer, Berlin, 2004, vol. 233, pp. 91–122.
20 A. Muraoka, K. Boukheddaden, J. Linares and F. Varret, Two-dimensional Ising-like model with specific edge effects for spin-crossover nanoparticles: A Monte Carlo study, *Phys. Rev. B: Condens. Matter Mater. Phys.*, 2011, **84**, 054119.
21 C. Enachescu, M. Nishino, S. Miyashita, L. Stoleriu and A. Stancu, Monte Carlo Metropolis study of cluster evolution in spin-crossover solids within the framework of a mechanoelastic model, *Phys. Rev. B: Condens. Matter Mater. Phys.*, 2012, **86**, 054114.
22 X. Jiang, G. Hao, X. Wang, A. Mosey, X. Zhang, L. Yu, A. J. Yost, A. D. DiChiara, X. Cheng, J. Zhang, R. Cheng, X. Xu and P. A. Dowben, Tunable spin-state bistability in a spin crossover molecular complex, *J. Phys.: Condens. Matter*, 2019, **31**, 315401.
23 L. Kipgen, M. Bernien, S. Ossinger, F. Nickel, A. J. Britton, L. M. Arruda, H. Naggert, C. Luo, C. Lotze, H. Ryll, F. Radu, E. Schierle, E. Weschke, F. Tuczek and W. Kuch, Evolution of cooperativity in the spin transition of an iron (II) complex on a graphite surface, *Nat. Commun.*, 2018, **9**, 1–8.
24 T. K. Ekanayaka, H. Kurz, A. S. Dale, G. Hao, A. Mosey, E. Mishra, R. Cheng, B. Weber and P. A. Dowben, Probing

the unpaired Fe spins across the spin crossover of a coordination polymer, *Mater. Adv.*, 2021, **2**, 760–768.
25 S. A. Siddiqui, O. Domanov, E. Schafler, J. Vejpravova and H. Shiozawa, Synthesis and size-dependent spin crossover of coordination polymer [Fe(Htrz)2(trz)](BF4), *J. Mater. Chem. C*, 2021, **9**, 1077–1084.
26 W. Phonsri, P. Harding, L. Liu, S. G. Telfer, K. S. Murray, B. Moubaraki, T. M. Ross, G. N. Jameson and D. J. Harding, Solvent modified spin crossover in an iron (III) complex: phase changes and an exceptionally wide hysteresis, *Chem. Sci.*, 2017, **8**, 3949–3959.
27 J. C. Dias, B. Vieira, I. C. Santos, L. C. Pereira and V. da Gama, Synthesis and characterization of Fe (III)(3-CH3O-qsal)2 PF6·nH2O (n = 0, 2), *Inorg. Chim. Acta*, 2009, **362**, 2076–2079.
28 D. J. Harding, D. Sertphon, P. Harding, K. S. Murray, B. Moubaraki, J. D. Cashion and H. Adams, Fe (III) Quinolylsalicylaldimine complexes: A rare mixed-spin-state complex and abrupt spin crossover, *Chem. – Eur. J.*, 2013, **19**, 1082–1090.
29 B. J. Vieira, J. C. Dias, I. C. Santos, L. C. Pereira, V. da Gama and J. C. Waerenborgh, Thermal hysteresis in a spin-crossover FeIII quinolylsalicylaldimine complex, FeIII (5-Br-Qsal)2Ni(Dmit)2·solv: Solvent effects, *Inorg. Chem.*, 2015, **54**, 1354–1362.
30 T. Shimizu, Y. Komatsu, H. Kamihata, Y. H. Lee, A. Fuyuhiro, S. Iijima and S. Hayami, Photo-switchable spin-crossover iron (III) compound based on intermolecular interactions, *J. Inclusion Phenom. Macrocyclic Chem.*, 2011, **71**, 363–369.
31 I. Nemec, R. Herchel and Z. Trávníček, The relationship between the strength of hydrogen bonding and spin crossover behaviour in a series of iron (III) Schiff base complexes, *Dalton Trans.*, 2015, **44**, 4474–4484.
32 A. C. Bas, V. Shalabaeva, X. Thompson, L. Vendier, L. Salmon, C. Thibault, G. Molnár, L. Routaboul and A. Bousseksou, Effects of solvent vapor annealing on the crystallinity and spin crossover properties of thin films of [Fe(HB(tz)3)2], *C. R. Chim.*, 2019, **22**, 525–533.
33 X. P. Sun, R. J. Wei, Z. S. Yao and J. Tao, Solvent effects on the structural packing and spin-crossover properties of a mononuclear iron (II) complex, *Cryst. Growth Des.*, 2018, **18**, 6853–6862.
34 M. A. Ribeiro, D. E. Stasiw, P. Pattison, P. R. Raithby, D. A. Shultz and C. B. Pinheiro, Toward controlling the solid state valence tautomeric interconversion character by solvation, *Cryst. Growth Des.*, 2016, **16**, 2385–2393.
35 K. Dankhoff, C. Lochenie, F. Puchtler and B. Weber, Solvent Influence on the Magnetic Properties of Iron(II) Spin-Crossover Coordination Compounds with 4,4′-Dipyridylethyne as Linker, *Eur. J. Inorg. Chem.*, 2016, 2136–2143.
36 R. Nowak, W. Bauer, T. Ossiander and B. Weber, Slow Self-Assembly Favors Hysteresis above Room Temperature for an Iron(II) 1D-Chain Spin-Crossover Complex, *Eur. J. Inorg. Chem.*, 2013, 975–983.
37 G. Hao, A. Mosey, X. Jiang, A. J. Yost, K. R. Sapkota, G. T. Wang, X. Zhang, J. Zhang, A. T. N'Diaye, R. Cheng, X. Xu and P. A. Dowben, Nonvolatile voltage controlled molecular spin state switching, *Appl. Phys. Lett.*, 2019, **114**, 032901.
38 A. Mosey, A. S. Dale, G. Hao, A. T. N'Diaye, P. A. Dowben and R. Cheng, Quantitative study of the energy changes in voltage-controlled spin crossover molecular thin films, *J. Phys. Chem. Lett.*, 2020, **11**, 8231–8237.
39 T. K. Ekanayaka, G. Hao, A. Mosey, A. S. Dale, X. Jiang, A. J. Yost, K. R. Sapkota, G. T. Wang, J. Zhang, A. T. N'Diaye, A. Marshall, R. Cheng, A. Naeemi, X. Xu and P. A. Dowben, Nonvolatile voltage controlled molecular spin-state switching for memory applications, *Magnetochemistry*, 2021, **7**, 37.
40 S. Cobo, G. Molnár, J. A. Real and A. Bousseksou, Multilayer sequential assembly of thin films that display room temperature spin crossover with hysteresis, *Angew. Chem., Int. Ed.*, 2006, **45**, 5786–5789.
41 G. Molnár, S. Cobo, J. A. Real, F. Carcenac, E. Daran, C. Vieu and A. Bousseksou, A combined top-down/bottom-up approach for the nanoscale patterning of spin-crossover coordination polymers, *Adv. Mater.*, 2007, **19**, 2163–2167.
42 X. Zhang, S. Mu, G. Chastanet, N. Daro, T. Palamarciuc, P. Rosa, J. F. Létard, J. Liu, G. E. Sterbinsky, D. A. Arena, C. Etrillard, B. Kundys, B. Doudin and P. A. Dowben, Complexities in the molecular spin crossover transition, *J. Phys. Chem. C*, 2015, **119**, 16293–16302.
43 C. Etrillard, V. Faramarzi, J. F. Dayen, J. F. Letard and B. Doudin, Photoconduction in [Fe $(Htrz)_2(trz)](BF_4)\cdot H_2O$ nanocrystals, *Chem. Commun.*, 2011, **47**, 9663–9665.
44 F. Guillaume, Y. A. Tobon, S. Bonhommeau, J. F. Létard, L. Moulet and E. Freysz, Photoswitching of the spin crossover polymeric material [Fe(Htrz)2(trz)](BF4) under continuous laser irradiation in a Raman scattering experiment, *Chem. Phys. Lett.*, 2014, **604**, 105–109.
45 M. A. Halcrow, Structure: function relationships in molecular spin-crossover complexes, *Chem. Soc. Rev.*, 2011, **40**, 4119–4142.
46 J. F. Létard, P. Guionneau and L. Goux-Capes, Towards spin crossover applications, *Spin Crossover in Transition Metal Compounds III*, Springer, Berlin, 2004, vol. 235, pp. 221–249.
47 O. Sato, J. Tao and Y. Z. Zhang, Control of magnetic properties through external stimuli, *Angew. Chem., Int. Ed.*, 2007, **46**, 2152–2187.
48 J. J. Lee, H. S. Sheu, C. R. Lee, J. M. Chen, J. F. Lee, C. C. Wang, C. H. Huang and Y. Wang, X-ray absorption spectroscopic studies on light-induced excited spin state trapping of an Fe (II) complex, *J. Am. Chem. Soc.*, 2000, **122**, 5742–5747.
49 T. G. Gopakumar, M. Bernien, H. Naggert, F. Matino, C. F. Hermanns, A. Bannwarth, S. Mühlenberend, A. Krüger, D. Krüger, F. Nickel, W. Walter, R. Berndt, W. Kuch and F. Tuczek, Spin-Crossover Complex on Au (111): Structural and Electronic Differences Between

Mono-and Multilayers, *Chem. – Eur. J.*, 2013, **19**, 15702–15709.

50 J. F. Létard, G. Chastanet, P. Guionneau and C. Desplanches, Optimizing the stability of trapped metastable spin states, in *Spin-crossover materials: Properties and applications*, ed. M. A. Halcrow, John Wiley & Sons, Hoboken, 1st edn, 2013, ch. 19, pp. 475–506.

51 C. Baldé, W. Bauer, E. Kaps, S. Neville, C. Desplanches, G. Chastanet, B. Weber and J. F. Létard, Light-Induced Excited Spin-State Properties in 1D Iron(II) Chain Compounds, *Eur. J. Inorg. Chem.*, 2013, 2744–2750.

52 A. Mohamed, M. Lee, K. Kitase, T. Kitazawa, J. Y. Kim and D. Y. Cho, Soft X-ray Absorption Spectroscopy Study of Spin Crossover Fe-Compounds: Persistent High Spin Configurations under Soft X-ray Irradiation, *Crystals*, 2018, **8**, 433.

53 D. Collison, C. D. Garner, C. M. McGrath, J. F. W. Mosselmans, M. D. Roper, J. M. W. Seddon, E. Sinn and N. A. Young, Soft X-ray induced excited spin state trapping and soft X-ray photochemistry at the iron L 2, 3 edge in [Fe (phen)$_2$(NCS)$_2$] and [Fe(phen)$_2$(NCSe)$_2$](phen= 1, 10-phenanthroline), *J. Chem. Soc., Dalton Trans.*, 1997, 4371–4376.

54 L. Poggini, M. Gonidec, J. H. González-Estefan, G. Pecastaings, B. Gobaut and P. Rosa, Vertical tunnel junction embedding a spin crossover molecular film, *Adv. Electron. Mater.*, 2018, **4**, 1800204.

55 B. Rösner, M. Milek, A. Witt, B. Gobaut, P. Torelli, R. H. Fink and M. M. Khusniyarov, Reversible Photoswitching of a Spin-Crossover Molecular Complex in the Solid State at Room Temperature, *Angew. Chem.*, 2015, **127**, 13168–13172.

56 Y. Hasegawa, S. Kume and H. Nishihara, Reversible light-induced magnetization change in an azobenzene-attached pyridylbenzimidazole complex of iron(II) at room temperature, *Dalton Trans.*, 2009, 280–284.

57 K. Takahashi, Y. Hasegawa, R. Sakamoto, M. Nishikawa, S. Kume, E. Nishibori and H. Nishihara, Solid-State Ligand-Driven Light-Induced Spin Change at Ambient Temperatures in Bis(dipyrazolylstyrylpyridine)iron(II) Complexes, *Inorg. Chem.*, 2012, **51**, 5188–5198.

58 M. Milek, F. W. Heinemann and M. M. Khusniyarov, Spin Crossover Meets Diarylethenes: Efficient Photoswitching of Magnetic Properties in Solution at Room Temperature, *Inorg. Chem.*, 2013, **52**, 11585–11592.

59 C. Lochenie, K. Schötz, F. Panzer, H. Kurz, B. Maier, F. Puchtler, S. Agarwal, A. Köhler and B. Weber, Spin-crossover iron (II) coordination polymer with fluorescent properties: correlation between emission properties and spin state, *J. Am. Chem. Soc.*, 2018, **140**, 700–709.

60 B. Weber, R. Tandon and D. Himsl, Synthesis, Magnetic Properties and X-ray Structure Analysis of a 1-D Chain Iron(II) Spin Crossover Complex with wide Hysteresis, *Z. Anorg. Allg. Chem.*, 2007, **633**, 1159–1162.

61 B. Weber, E. Kaps, C. Desplanches and J. F. Létard, Quenching the Hysteresis in Single Crystals of a 1D Chain Iron(II) Spin Crossover Complex, *Eur. J. Inorg. Chem.*, 2008, 2963–2966.

62 C. Lochenie, A. Gebauer, O. Klimm, F. Puchtler and B. Weber, Iron (ii) spin crossover complexe with diaminonaphthalene-based Schiff base-like ligands: 1D coordination polymers, *New J. Chem.*, 2016, **40**, 4687–4695.

63 J. Kroeber, J. Audière, R. Claude, E. Codjovi, O. Kahn, J. G. Haasnoot, F. Groliere, C. Jay and A. Bousseksou, Spin transitions and thermal hysteresis in the molecular-based materials [Fe(Htrz)$_2$(trz)](BF$_4$) and [Fe(Htrz)$_3$](BF$_4$)$_2$·H$_2$O (Htrz = 1,2,4-4H-triazole; trz = 1,2,4-triazolato), *Chem. Mater.*, 1994, **6**, 1404–1412.

64 C. Lochenie, W. Bauer, A. P. Railliet, S. Schlamp, Y. Garcia and B. Weber, Large Thermal hysteresis for Iron (II) spin crossover complexes with N-(Pyrid-4-Yl) Isonicotinamide, *Inorg. Chem.*, 2014, **53**, 11563–11572.

65 S. Beniwal, X. Zhang, S. Mu, A. Naim, P. Rosa, G. Chastanet, L. F. Létard, J. Liu, G. E. Sterbinsky, D. A. Arena and P. A. Dowben, Surface-induced spin state locking of the [Fe (H2B(pz)2)2(bipy)] spin crossover complex, *J. Phys.: Condens. Matter*, 2016, **28**, 206002.

66 S. I. Ohkoshi, K. Imoto, Y. Tsunobuchi, S. Takano and H. Tokoro, Light-induced spin-crossover magnet, *Nat. Chem.*, 2011, **3**, 564–569.

67 H. Naggert, A. Bannwarth, S. Chemnitz, T. von Hofe, E. Quandt and F. Tuczek, First observation of light-induced spin change in vacuum deposited thin films of iron spin crossover complexes, *Dalton Trans.*, 2011, **40**, 6364–6366.

68 V. Ksenofontov, A. B. Gaspar, G. Levchenko, B. Fitzsimmons and P. Gütlich, Pressure effect on spin crossover in [Fe(phen)2(NCS)2] and [CrI2(depe)2], *J. Phys. Chem. B*, 2004, **108**, 7723–7727.

69 T. Miyamachi, M. Gruber, V. Davesne, M. Bowen, S. Boukari, L. Joly, F. Scheurer, G. Rogez, T. K. Yamada, P. Ohresser and E. Beaurepaire, Robust spin crossover and memristance across a single molecule, *Nat. Commun.*, 2012, **3**, 1–6.

70 X. Zhang, X. Jiang, X. Zhang, Y. Yin, X. Chen, X. Hong, X. Xu and P. A. Dowben, Indications of magnetic coupling effects in spin cross-over molecular thin films, *Chem. Commun.*, 2018, **54**, 944–947.

71 X. Zhang, T. Palamarciuc, J. F. Letard, P. Rosa, E. V. Lozada, F. Torres, L. G. Rosa, B. Doudin and P. A. Dowben, The spin state of a molecular adsorbate driven by the ferroelectric substrate polarization, *Chem. Commun.*, 2014, **50**, 2255.

72 T. G. Gopakumar, F. Matino, H. Naggert, A. Bannwarth, F. Tuczek and R. Berndt, Electron-induced spin crossover of single molecules in a bilayer on gold, *Angew. Chem., Int. Ed.*, 2012, **51**, 6262–6266.

73 T. Mahfoud, G. Molnár, S. Bonhommeau, S. Cobo, L. Salmon, P. Demont, H. Tokoro, S. I. Ohkoshi, K. Boukheddaden and A. Bousseksou, Electric-field-induced charge-transfer phase transition: A promising

approach toward electrically switchable devices, *J. Am. Chem. Soc.*, 2009, **131**, 15049–15054.

74 X. Zhang, P. S. Costa, J. Hooper, D. P. Miller, A. T. N'Diaye, S. Beniwal, X. Jiang, Y. Yin, P. Rosa, L. Routaboul, M. Gonidec, L. Poggini, P. Braunstein, B. Doudin, X. Xu, A. Enders, E. Zurek and P. A. Dowben, Locking and unlocking the molecular spin crossover transition, *Adv. Mater.*, 2017, **29**, 1702257.

75 A. R. Craze, K. J. Howard-Smith, M. M. Bhadbhade, O. Mustonen, C. J. Kepert, C. E. Marjo and F. Li, Investigation of the High-Temperature Spin-Transition of a Mononuclear Iron (II) Complex Using X-ray Photoelectron Spectroscopy, *Inorg. Chem.*, 2018, **57**, 6503–6510.

76 J. Y. Son, K. Takubo, D. Asakura, J. W. Quilty, T. Mizokawa, A. Nakamoto and N. Kojima, Photoemission study of temperature-induced and photoinduced spin-state transitions in spin-crossover complex [Fe (ptz)6](BF4)2, *J. Phys. Soc. Jpn.*, 2007, **76**, 084703.

77 L. Poggini, M. Milek, G. Londi, A. Naim, G. Poneti, L. Squillantini, A. Magnani, F. Totti, P. Rosa, M. M. Khusniyarov and M. Mannini, Room temperature control of spin states in a thin film of a photochromic iron (II) complex, *Mater. Horiz.*, 2018, **5**, 506–513.

78 A. Pronschinske, R. C. Bruce, G. Lewis, Y. Chen, A. Calzolari, M. Buongiorno-Nardelli, D. A. Shultz, W. You and D. B. Dougherty, Iron (II) spin crossover films on Au (111): scanning probe microscopy and photoelectron spectroscopy, *Chem. Commun.*, 2013, **49**, 10446–10452.

79 M. A. Halcrow, Manipulating metal spin states for biomimetic, catalytic and molecular materials chemistry, *Dalton Trans.*, 2020, **49**, 15560.

80 B. Warner, J. C. Oberg, T. G. Gill, F. El Hallak, C. F. Hirjibehedin, M. Serri, S. Heutz, M. A. Arrio, P. Sainctavit, M. Mannini, G. Poneti, R. Sessoli and P. Rosa, Temperature-and light-induced spin crossover observed by x-ray spectroscopy on isolated Fe (II) complexes on gold, *J. Phys. Chem. Lett.*, 2013, **4**, 1546–1552.

81 X. Zhang, T. Palamarciuc, P. Rosa, J. F. Létard, B. Doudin, Z. Zhang, J. Wang and P. A. Dowben, Electronic structure of a spin crossover molecular adsorbate, *J. Phys. Chem. C*, 2012, **116**, 23291–23296.

82 M. Bernien, H. Naggert, L. M. Arruda, L. Kipgen, F. Nickel, J. Miguel, C. F. Hermanns, A. Krüger, D. Krüger, E. Schierle, E. Weschke, F. Tuczek and W. Kuch, Highly efficient thermal and light-induced spin-state switching of an Fe (II) complex in direct contact with a solid surface, *ACS Nano*, 2015, **9**, 8960–8966.

83 M. Bernien, D. Wiedemann, C. F. Hermanns, A. Krüger, D. Rolf, W. Kroener, P. Müller, A. Grohmann and W. Kuch, Spin crossover in a vacuum-deposited submonolayer of a molecular iron (II) complex, *J. Phys. Chem. Lett.*, 2012, **3**, 3431–3434.

84 V. Briois, C. C. dit Moulin, P. Sainctavit, C. Brouder and A. M. Flank, Full multiple scattering and crystal field multiplet calculations performed on the spin transition FeII (phen)2(NCS)2 complex at the iron K and L2,3 X-ray absorption edges, *J. Am. Chem. Soc.*, 1995, **117**, 1019–1026.

85 D. Collison, C. D. Garner, C. M. McGrath, J. F. W. Mosselmans, M. D. Roper, J. M. Seddon, E. Sinn and N. A. Young, Soft x-ray induced excited spin state trapping and soft X-ray photochemistry at the iron L2,3 edge in [Fe(phen)2(NCS)2] and [Fe(phen)2(NCSe)2](phen= 1, 10-phenanthroline), *J. Chem. Soc., Dalton Trans.*, 1997, 4371–4376.

86 M. Gruber, T. Miyamachi, V. Davesne, M. Bowen, S. Boukari, W. Wulfhekel, M. Alouani and E. Beaurepaire, Spin crossover in Fe(phen)2 (NCS)2 complexes on metallic surfaces, *J. Chem. Phys.*, 2017, **146**, 092312.

87 S. Schönfeld, W. Bauer, S. Thallmair, G. Hörner and B. Weber, Running in the Family: Molecular Factors controlling Spin Crossover of Iron(II) Complexes with Schiff-base like Ligands, *Z. Anorg. Allg. Chem.*, 2021, **647**, 905–914.

88 S. Schönfeld, K. Dankhoff, D. Baabe, M. K. Zaretzke, M. Bröring, K. Schötz, A. Köhler, G. Hörner and B. Weber, Iron(II) Spin Crossover Complexes Based on a Redox Active Equatorial Schiff-Base-Like Ligand, *Inorg. Chem.*, 2020, **59**, 8320–8333.

89 S. Beniwal, S. Sarkar, F. Baier, B. Weber, P. A. Dowben and A. Enders, Site selective adsorption of the spin crossover complex $Fe(phen)_2(NCS)2$ on Au (111), *J. Phys.: Condens. Matter*, 2020, **32**, 324003.

90 E. C. Ellingsworth, B. Turner and G. Szulczewski, Thermal conversion of $[Fe(phen)_3](SCN)_2$ thin films into the spin crossover complex $Fe(phen)_2(NCS)_2$, *RSC Adv.*, 2013, **3**, 3745–3754.

91 M. Marchivie, P. Guionneau, J. A. Howard, G. Chastanet, J. F. Létard, A. E. Goeta and D. Chasseau, Structural Characterization of a Photoinduced Molecular Switch, *J. Am. Chem. Soc.*, 2002, **124**, 194–195.

92 R. P. Gupta and S. K. Sen, Calculation of multiplet structure of core p-vacancy levels. II, *Phys. Rev. B: Solid State*, 1975, **12**, 15.

93 A. P. Grosvenor, B. A. Kobe, M. C. Biesinger and N. S. McIntyre, Investigation of multiplet splitting of Fe 2p XPS spectra and bonding in iron compounds, *Surf. Interface Anal.*, 2004, **36**, 1564.

94 A. E. Bocquet, T. Mizokawa, T. Saitoh, H. Namatame and A. Fujimori, Electronic structure of 3d-transition-metal compounds by analysis of the 2p core-level photoemission spectra, *Phys. Rev. B: Condens. Matter Mater. Phys.*, 1992, **46**, 3771.

95 S. Cao, T. R. Paudel, K. Sinha, X. Jiang, W. Wang, E. Y. Tsymbal, X. Xu and P. A. Dowben, The stability and surface termination of hexagonal $LuFeO_3$, *J. Phys.: Condens. Matter*, 2015, **27**, 175004.

96 C. D. Bain and G. M. Whitesides, Attenuation Lengths of Photoelectrons in Hydrocarbon Films, *J. Phys. Chem.*, 1989, **93**, 1670–1673.

97 P.-L. Girard-Lauriault, T. Gross, A. Lippitz and W. E. S. Unger, Chemical and Elemental Depth Profiling of Very Thin Organic Layers by Constant Kinetic Energy XPS: A New Synchrotron XPS Analysis Strategy, *Anal. Chem.*, 2012, **84**, 5984–5991.
98 A. Jablonski and C. J. Powell, The electron attenuation length revistied, *Surf. Sci. Rep.*, 2002, **47**, 33–41.
99 M. P. Seah and W. A. Dench, Quantitative Electron Spectroscopy of Surfaces: A standard Data Base for Electron Inelastic Mean Free Paths in Solids, *Surf. Interface Anal.*, 1979, **1**, 2–11.
100 D. R. Penn, Eelctron Mean Free Path calculations using a model dielectric function, *Phys. Rev. B: Condens. Matter Mater. Phys.*, 1987, **35**, 482–486.
101 Ö. Üngör, E. S. Choi and M. Shatruk, Optimization of crystal packing in semiconducting spin-crossover materials with fractionally charged $TCNQ^{\delta-}$ anions ($0 < \delta < 1$), *Chem. Sci.*, 2021, **12**, 10765–10779.

